DOE/ER/14079--2

DE91 001445

Stable Explicit Depth Extrapolation of Seismic Wavefields

by

Dave Hale

Center for Wave Phenomena
Colorado School of Mines
Golden, Colorado 80401
Phone (303) 273-3557

Stable explicit depth extrapolation of seismic wavefields

Dave Hale

ABSTRACT

Stability has traditionally been one of the most compelling advantages of implicit methods for seismic wavefield extrapolation. The common 45-degree finite-difference migration algorithm, for example, is based on an implicit wavefield extrapolation that is guaranteed to be stable. Specifically, wavefield energy will not grow exponentially with depth as the wavefield is extrapolated backwards into the subsurface. Explicit methods, in contrast, tend to be unstable. Without special care, numerical deficiencies in explicit extrapolation methods cause wavefield energy to grow exponentially with depth, contrary to physical expectations.

The Taylor series method may be used to design finite-length, explicit, extrapolation filters. In the usual Taylor series method, N coefficients of a finite-length filter are chosen to match N terms in a truncated Taylor series approximation of the desired filter's Fourier transform. This method always yields unstable extrapolation filters. However, a simple modification of the Taylor series method yields extrapolators that are unconditionally stable.

The accuracy of stable explicit extrapolators is determined by their length—longer extrapolators yield accurate extrapolation for a wider range of propagation angles than do shorter filters. Because an infinitely long extrapolator is required to extrapolate waves propagating at angles approaching 90 degrees, stable explicit extrapolators may be less efficient than implicit extrapolators for high propagation angles. For more modest propagation angles of 50 degrees or less, stable explicit extrapolators are more efficient than modern implicit extrapolators. Furthermore, unlike implicit extrapolators, stable explicit extrapolators naturally attenuate waves propagating at high angles for which the extrapolators are inaccurate.

INTRODUCTION

Implicit filtering methods are widely used to extrapolate seismic wavefields in depth. For example, the well-known 45-degree finite-difference method for depth migration is based on a recursive application of implicit filtering (e.g., Claerbout, 1985). Implicit methods are most attractive because they are guaranteed to be stable. Specifically, implicit methods for depth extrapolation will not permit the amplitude of the extrapolated wavefield to grow with depth. In contrast, the most straightforward explicit extrapolation methods are unstable, tending to amplify wavefield amplitudes exponentially with depth.

Notwithstanding stability, explicit filtering is attractive because it resembles convolution, for which each filtered output sample can be computed independently, perhaps in parallel with other output samples. Implicit filtering, in contrast, is accomplished by solving a linear system of coupled equations for the filtered output samples. Partly because it is simpler, explicit filtering is likely to be more efficiently implemented on various computers than is implicit filtering.

In addition to simplicity, another advantage shared by explicit methods for depth extrapolation of seismic wavefields is the ease with which explicit methods can be extended for use in 3-D depth migration. The solution of linear system of equations required by implicit methods is particularly awkward in this application. For example, an accurate extension of the implicit 45-degree finite-difference method to 3-D depth migration is difficult and may be computationally impractical (Claerbout, 1985, p. 101; Yilmaz, 1987, p. 405). Explicit depth extrapolation methods, in contrast, are easily extended to 3-D depth migration, as demonstrated by Blacquière et al (1989).

These advantages of computational simplicity, efficiency, and extendability motivate the development of a method for designing *stable* explicit depth extrapolation filters. In addition to discussing these advantages, Holberg (1988) describes a constrained least-squares method for designing extrapolation filters that he claims are "unconditionally stable". However, amplitude spectra of these filters suggest that this claim is not strictly valid. Although Holberg's design method may be useful in practice, repeated application of Holberg's extrapolation filters results in exponential growth of amplitudes for certain frequencies (and wavenumbers) in the seismic wavefield.

In the spirit of Holberg's work, this paper addresses the following filter design problem:

> *Find N coefficients h_n of a finite-length filter with a Fourier transform $H(k)$ that approximates the desired Fourier transform defined by*
>
> $$D(k) \equiv e^{i\frac{\Delta z}{\Delta x}\left[\left(\frac{\omega\Delta x}{v}\right)^2-k^2\right]^{1/2}}, \qquad (1)$$
>
> *for $|k| \le |\omega\Delta x/v|$, subject to the constraint that $|H(k)| \le 1$ for $|k| \le \pi$.*

In the definition of $D(k)$, ω denotes frequency (in radians per unit time), v denotes velocity, and Δz and Δx denote vertical and horizontal spatial sampling intervals,

respectively. Wavenumber k (measured in radians per sample in the x direction) is normalized such that any distance quantity is measured in terms of the number of horizontal sampling intervals Δx. With this normalization, two dimension-less constants, $\Delta z/\Delta x$ and $\omega \Delta x/v$, uniquely determine the desired transform $D(k)$.

The desired transform $D(k)$ defined by equation (1) is appropriate for waves traveling one way, either down or up. In depth extrapolation of CMP stacked data, which corresponds to waves propagating both down and up, we may use the "exploding reflectors" concept and replace velocity v with half-velocity $v/2$ (e.g., Claerbout, 1985). This replacement is implied by references to half-velocity below. The symmetry of the desired transform $D(k)$ with respect to k implies that the complex extrapolation filter coefficients h_n should be even. Specifically, we expect $h_{-n} = h_n$. Therefore, the number of coefficients N should be odd, with the coefficient index n bounded by $-(N-1)/2 \le n \le (N-1)/2$.

EXPLICIT EXTRAPOLATORS FOR A SINGLE FREQUENCY

Figure 1 illustrates amplitude spectra $|H(k)|$ for three explicit, 19-coefficient extrapolators, as a function of normalized wavenumber (measured in cycles). In this example, $\Delta z = \Delta x$ and normalized frequency $\omega \Delta x/v = \pi/2$ radians. Therefore, the right half of this figure corresponds to evanescent waves for which $|k| > |\omega \Delta x/v|$.

The light gray curve corresponds to an extrapolator designed by an unconstrained least-squares method, which is equivalent to simply inverse Fourier transforming the desired transform $D(k)$ and truncating to the desired number of coefficients $N = 19$. The amplitude spectrum of this extrapolator has a ripply character that is typical of filters designed by least-squares methods. Note that the amplitude is greater than one for some wavenumbers; Fourier components of a seismic wavefield corresponding to these wavenumbers will grow exponentially as this extrapolator is applied repeatedly in the recursive process of depth extrapolation.

The dark gray curve in Figure 1 corresponds to an extrapolator that was designed by a conventional Taylor series method, in which the $N = 19$ coefficients were chosen to match $N = 19$ terms in a truncated Taylor series approximation of the desired $D(k)$. (See Appendix A.) As the amplitude spectrum indicates, this extrapolator is quite unstable, particularly for the evanescent wavenumbers.

The black curve in Figure 1 corresponds to a 19-coefficient extrapolator that was designed by a modified Taylor series method described in Appendix A. Because this extrapolator has no amplitudes greater than one, it is stable for all wavenumbers. Note that this extrapolator attenuates high wavenumbers, with most of the attenuation occuring in the evanescent region.

Figure 2 is a detailed plot of the amplitude errors for the three extrapolators. As noted above, the ripply character of the least-squares (light gray) extrapolator is typical. However, Holberg (1988) has demonstrated that the magnitude of these oscillations can be significantly reduced (1) by restricting the range of wavenumbers for which the least-squares fit is attempted and (2) by constraining the filter to be stable

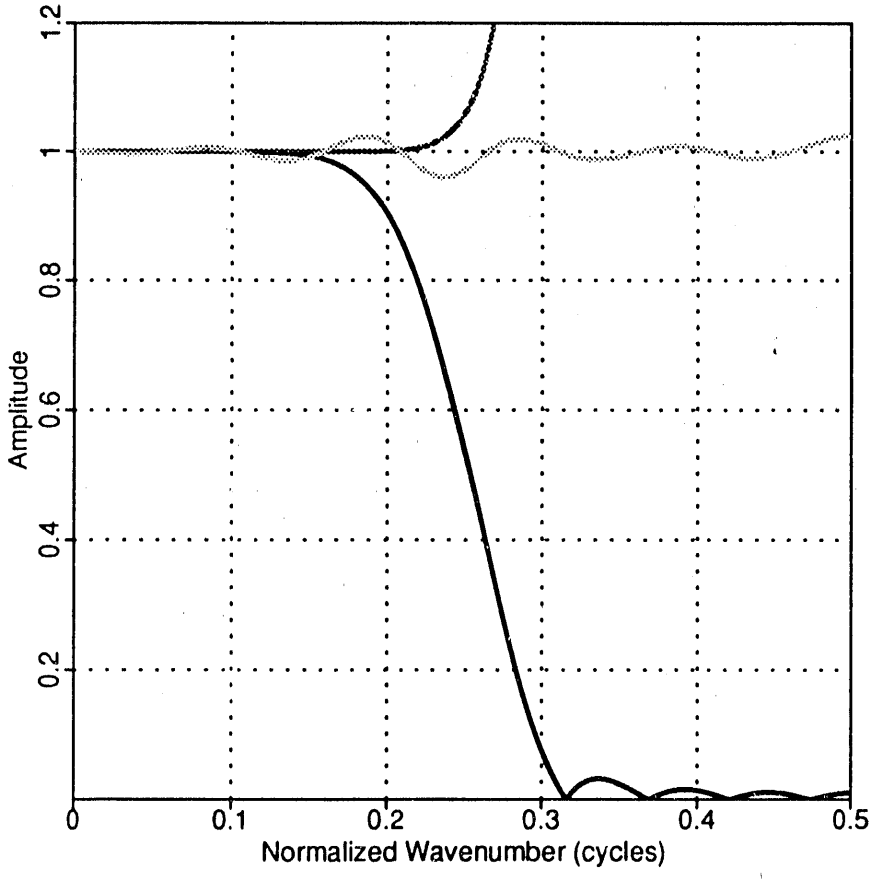

FIG. 1. Amplitude spectra for 19-coefficient explicit extrapolators designed by an unconstrained least-squares method (light gray), the conventional Taylor series method (dark gray), and the modified Taylor series method described in Appendix A (black). The ripply amplitude spectrum (light gray) is characteristic of least-squares filter designs. Smooth amplitude spectra (dark gray and black) are characteristic of Taylor series methods. Only the modified Taylor series method (black) yields an extrapolator stable for all wavenumbers. In this figure, normalized wavenumbers greater than 0.25 correspond to evanescent waves.

(amplitudes less than one) for wavenumbers *outside* this range. (Why was Holberg's constraint that amplitudes be less than one not enforced for *all* wavenumbers?) However, Holberg's extrapolators also exhibit oscillating amplitude errors, some of which are positive (amplitudes greater than one) within the range of wavenumbers over which the least-squares fit is attempted (Holberg, 1988, p. 108). Holberg's extrapolators have less amplitude error than the unconstrained least-squares extrapolators shown here, but they are not "unconditionally stable".

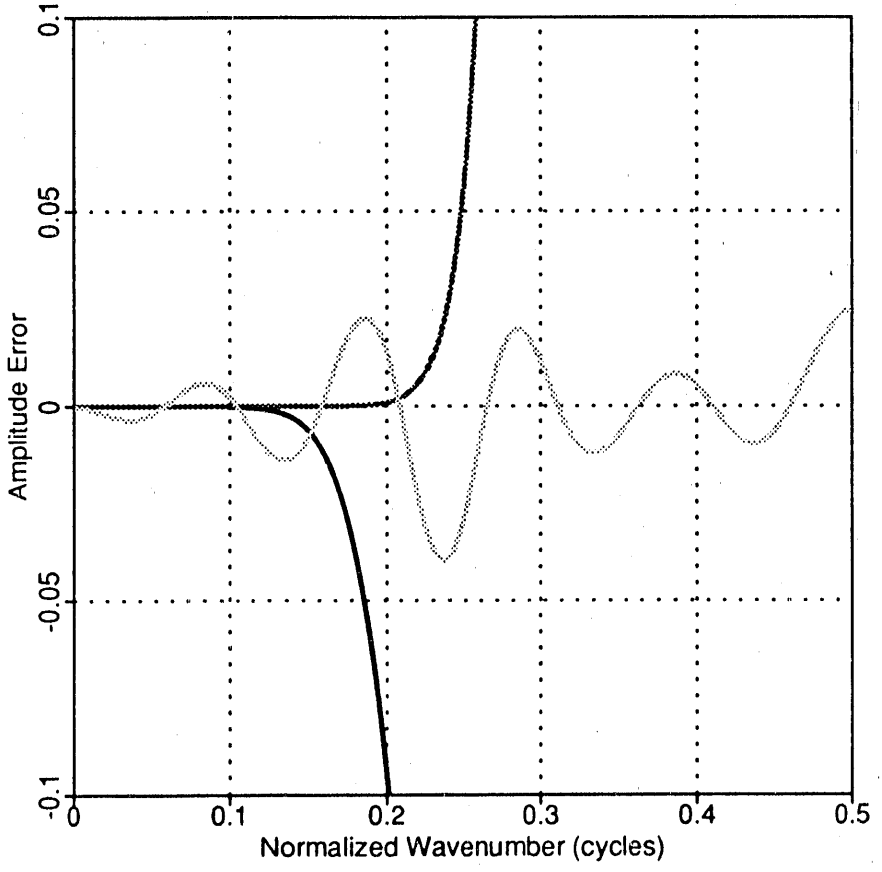

FIG. 2. Amplitude errors for 19-coefficient explicit extrapolators designed by an unconstrained least-squares method (light gray), the conventional Taylor series method (dark gray), and the modified Taylor series method described in Appendix A (black). Positive errors imply an unstable extrapolator. Only the modified Taylor series method (black) yields an extrapolator stable for all wavenumbers. In this figure, normalized wavenumbers greater than 0.25 correspond to evanescent waves.

Whereas amplitude errors in Figure 2 indicate stability (or instability), the phase errors plotted in Figures 3 and 4 indicate how well (or how poorly) explicit extrapolators will position reflectors in depth migration. The phase errors plotted in Figures 3 and 4 correspond to extrapolators with 19 and 39 coefficients, respectively. As expected, increasing the length of an extrapolator reduces its phase error.

Figures 3 and 4 suggest that a high price has been paid for stability. The stable extrapolator exhibits significantly greater phase error than either of the two unstable extrapolators.

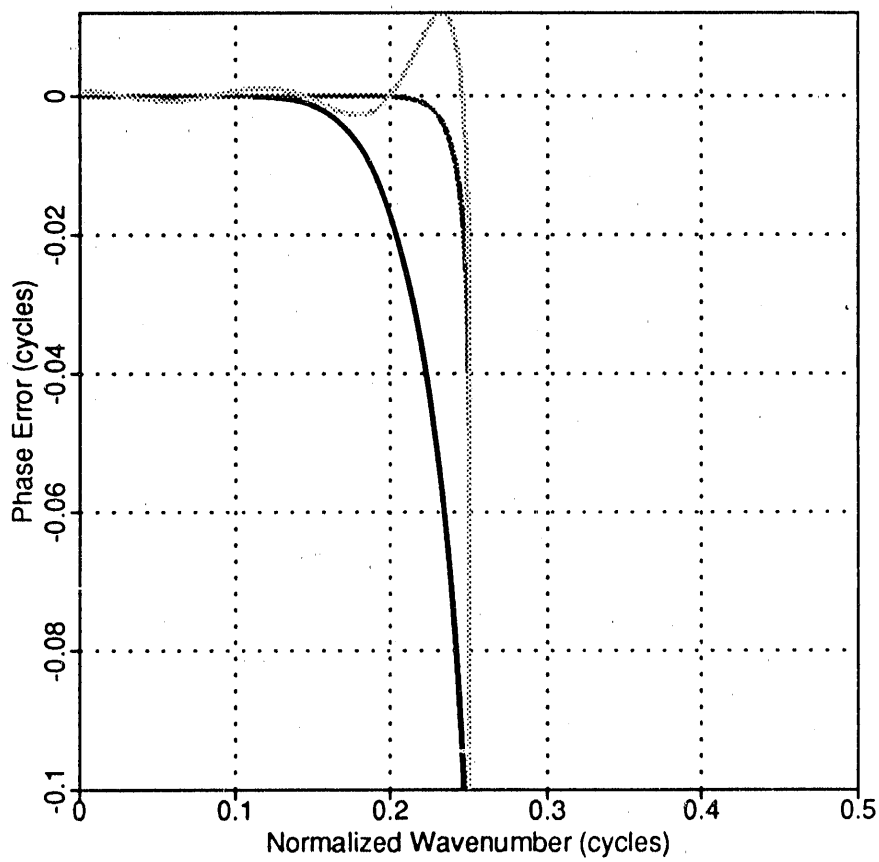

FIG. 3. Phase errors for 19-coefficient explicit extrapolators designed by an unconstrained least-squares method (light gray), the conventional Taylor series method (dark gray), and the modified Taylor series method described in Appendix A (black). Stable explicit extrapolators, such as that designed by the modified Taylor series method (black), exhibit greater phase error than do unstable extrapolators. In this figure, normalized wavenumbers greater than 0.25 correspond to evanescent waves.

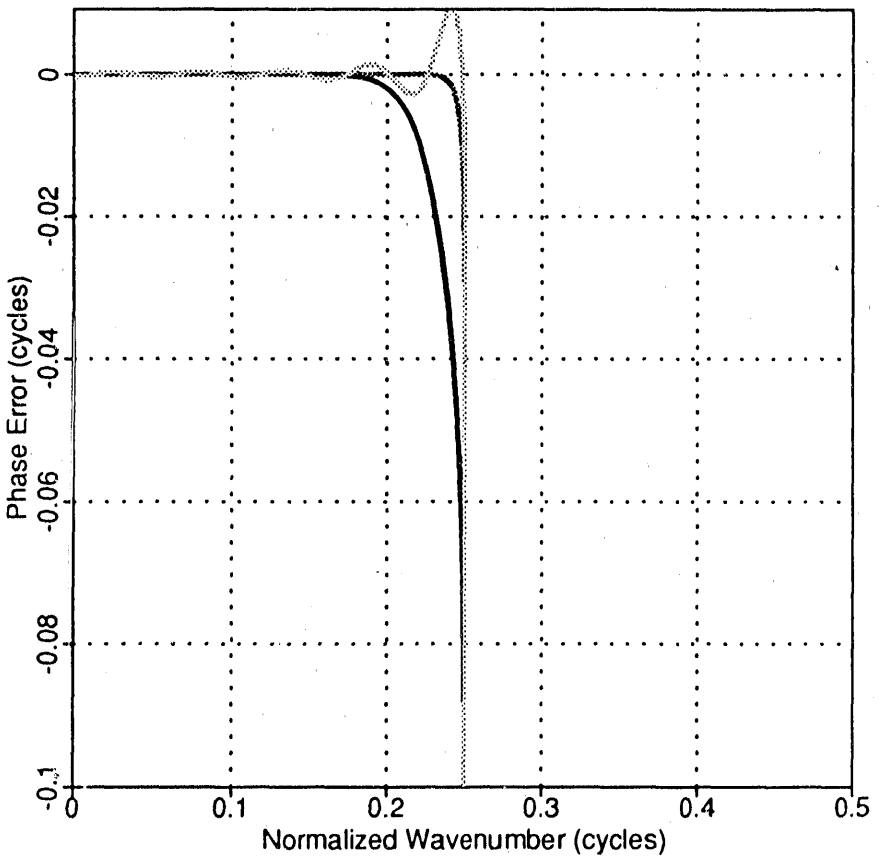

FIG. 4. Phase errors for 39-coefficient explicit extrapolators designed by an unconstrained least-squares method (light gray), the conventional Taylor series method (dark gray), and the modified Taylor series method described in Appendix A (black). Comparison with Figure 3 indicates that increasing the length of explicit extrapolators reduces phase error. In this figure, normalized wavenumbers greater than 0.25 correspond to evanescent waves.

EXPLICIT EXTRAPOLATORS FOR A RANGE OF FREQUENCIES

Figures 1 through 4 illustrate amplitude and phase errors of extrapolators designed for the particular normalized frequency $\omega\Delta x/v = \pi/2$ radians. In practice, extrapolation filters must be designed for a wide range of frequencies. Figures 5 and 6 show *contours* of amplitude and phase errors, respectively, for stable explicit extrapolators with 39 coefficients. Errors are plotted as a function of normalized frequency and wave propagation angle. As in the preceding examples, I chose $\Delta z = \Delta x$ in designing these stable extrapolators.

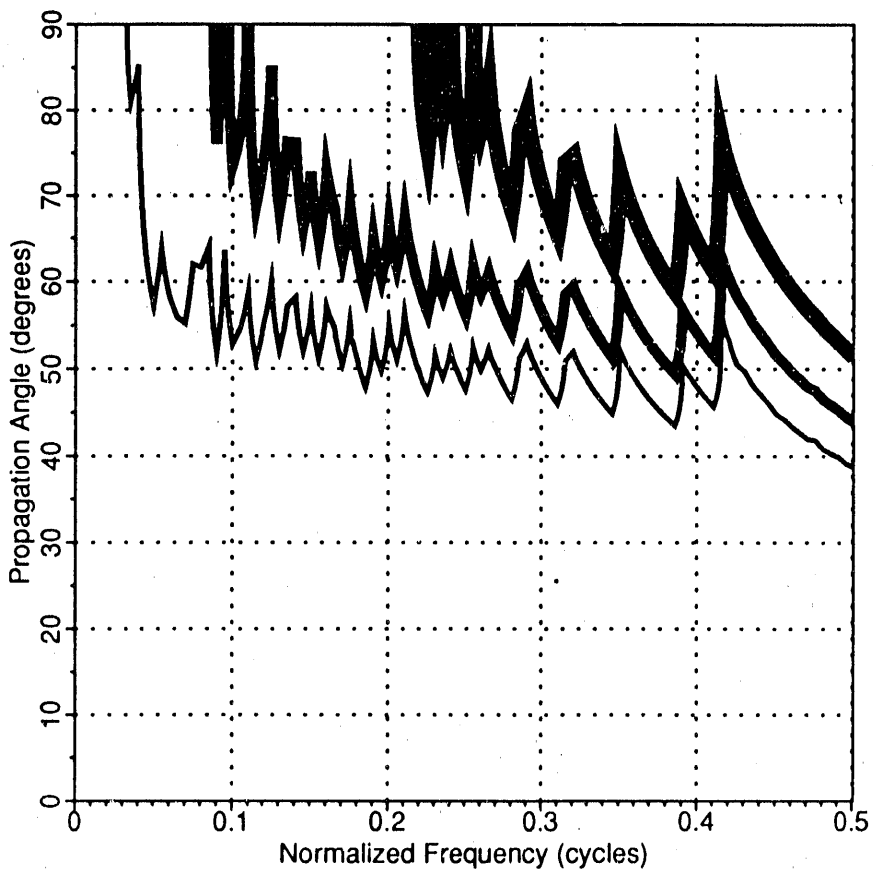

FIG. 5. Amplitude error for a 39-coefficient explicit extrapolator designed by the modified Taylor series method described in Appendix A. Error is contoured as a function of normalized frequency and propagation angle (measured from vertical). Normalized (dimension-less) frequency is frequency (Hz) times the horizontal sampling interval (km) divided by velocity (km/s). Contour values are $-1/1000$ (thin), $-1/100$ (medium), and $-1/10$ (thick).

For convenience in using these figures, the normalized frequency axis has been labeled in cycles (instead of radians), ranging from 0.0 to 0.5 cycles. For example, a frequency of 40 Hz, a CMP spacing of 12.5 m, and a velocity (or half-velocity) of 1 km/s correspond to a normalized frequency of 0.5 cycles. Normalized frequency can easily be computed for other choices of these parameters, and the computed values will typically fall inside the range 0.0 to 0.5 cycles.

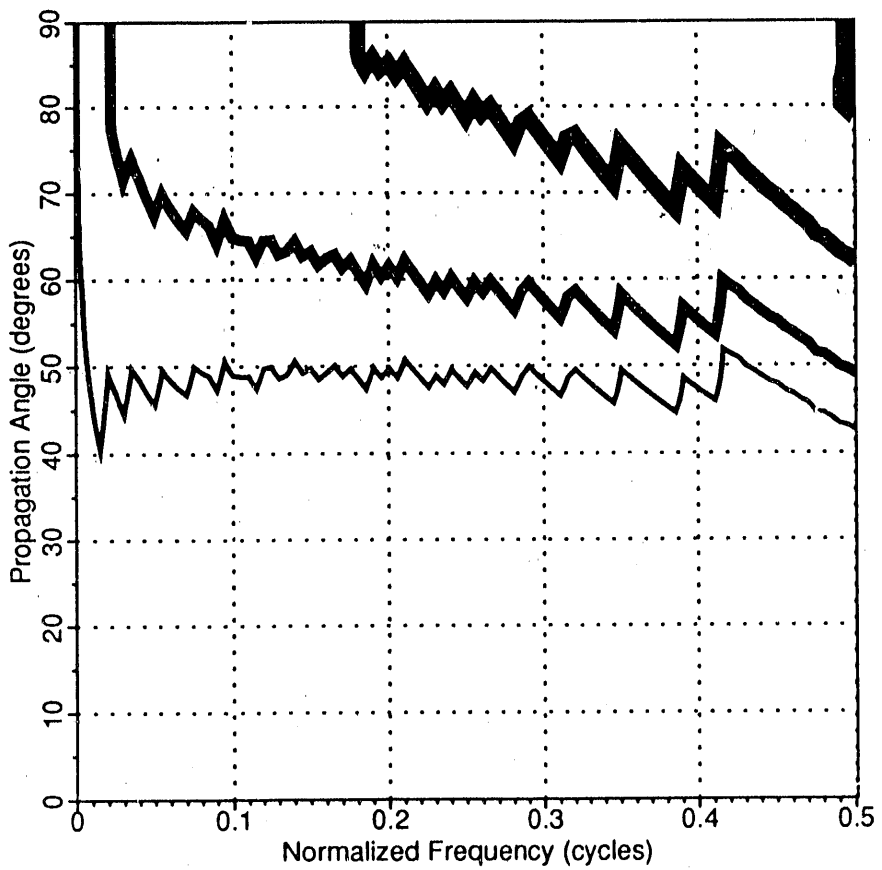

FIG. 6. Phase error for a 39-coefficient explicit extrapolator designed by the modified Taylor series method described in Appendix A. Error is contoured as a function of normalized frequency and propagation angle (measured from vertical). Normalized (dimension-less) frequency is frequency (Hz) times the horizontal sampling interval (km) divided by velocity (km/s). Contour values are $-\pi/1000$ (thin), $-\pi/100$ (medium), and $-\pi/10$ (thick).

Amplitude error for stable extrapolators is contoured in Figure 5 for errors of $-1/1000$, $-1/100$, and $-1/10$, corresponding to thin, medium, and thick contours, respectively. (Thick contours imply large errors.) Figure 5 shows that stable extrapolators will attenuate waves propagating at an angle of 50 degrees for most frequencies by a factor of 0.999 in one extrapolation step. After 1000 such extrapolation steps, these waves will have been attenuated by a factor of 0.999 raised to the 1000'th power, which is approximately $1/e \approx 0.37$.

Phase error for stable extrapolators is contoured in Figure 6 for errors of $-\pi/1000$, $-\pi/100$, and $-\pi/10$, corresponding to thin, medium, and thick contours, respectively. (Again, thick contours imply large errors.) Since phase errors accumulate, Figure 6 shows, for example, that these stable explicit extrapolators yield one-half cycle (π radians) of phase error after 1000 extrapolation steps for waves propagating at an angle of about 50 degrees. Comparison of Figures 5 and 6 suggests that waves propagating at very high angles will be attenuated, so that only those propagation angles for which the stable extrapolators are accurate will be preserved during depth extrapolation. In other words, a depth migration process based on these extrapolators will attenuate steeply dipping reflectors that would otherwise be mis-positioned due to large phase errors.

As suggested by Figures 3 and 4, the errors in stable explicit extrapolators may be reduced by using longer extrapolators. Likewise, shorter extrapolators yield greater errors. Although not shown here, a stable explicit extrapolator with 19 (instead of 39) coefficients yields one-half cycle of phase error after 1000 extrapolation steps for waves propagating at an angle of 35 degrees. Therefore, about 15 degrees of propagation angle may be gained by doubling (approximately) the number of extrapolator coefficients from 19 to 39.

Note that the phase error in Figure 6 is more or less independent of frequency. In contrast, the phase error for implicit depth extrapolation is highly frequency-dependent. For comparison, phase error for a so-called "65-degree" implicit extrapolation filter (Lee and Suh, 1985) is contoured in Figure 7. The term "65-degree" refers to the accuracy in approximating the square-root in equation 1. Specifically, the 65-degree approximation is obtained by a slight adjustment of the coefficients of the more traditional 45-degree approximation to the square-root. These terms fail to account for errors in approximating spatial derivatives with finite differences; these are the errors that account for the increase in phase error with increasing normalized frequency evident in Figure 7.

Recalling the definition above of normalized frequency, the only parameter that may be adjusted in practice to reduce this phase error is the horizontal spatial sampling interval Δx. For the previous example of a frequency of 40 Hz and a half-velocity of 1 km/s, Figure 7 implies that $\Delta x = 1.25$ m would be required to obtain less than one-half cycle of phase error after 1000 extrapolation steps for a wave propagating at 65 degrees. This spatial sampling interval is a factor of 10 smaller than the 12.5 m necessary to avoid spatial aliasing. Recalling that $\Delta z = \Delta x$ for the extrapolators shown here, the size of each vertical depth step must be reduced accordingly, which

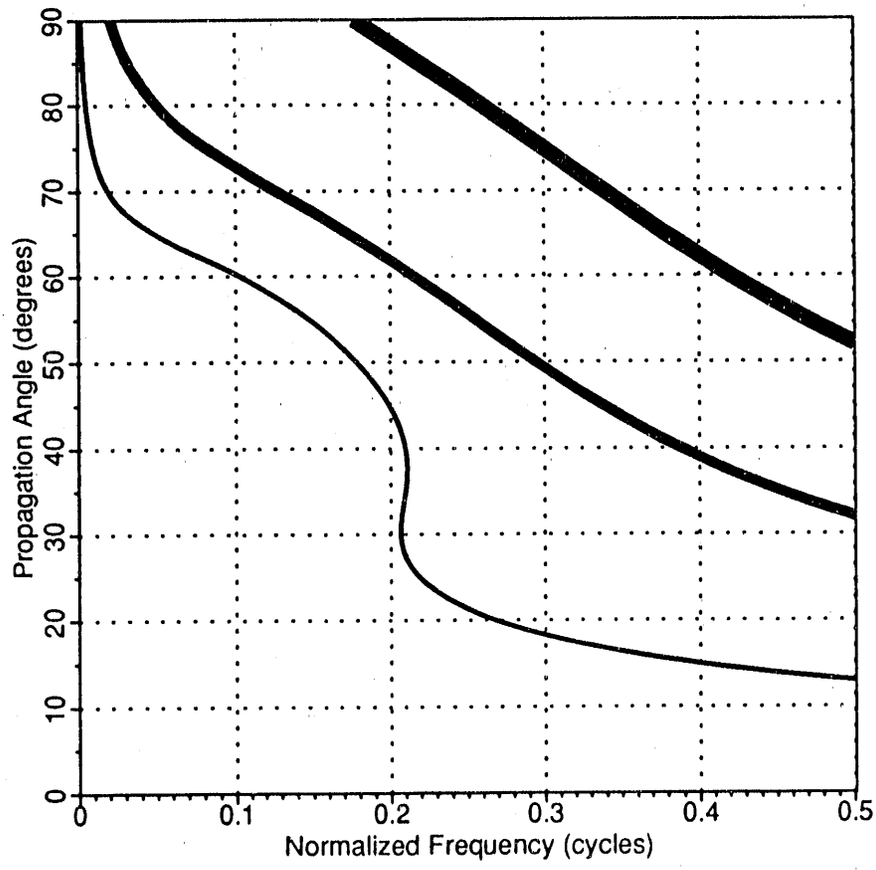

FIG. 7. Phase error for a so-called "65-degree" implicit extrapolator. Compare with Figure 6. Error is contoured as a function of normalized frequency and propagation angle (measured from vertical). Normalized (dimension-less) frequency is frequency (Hz) times the horizontal sampling interval (km) divided by velocity (km/s). Contour values are $-\pi/1000$ (thin), $-\pi/100$ (medium), and $-\pi/10$ (thick).

implies that more steps are necessary to extrapolate to a particular depth. In practice, the high computational cost associated with such fine spatial sampling intervals suggests that 65-degree accuracy is rarely achieved with 65-degree implicit methods for depth migration.

For those wishing to reproduce the errors contoured in Figure 7, horizontal spatial derivatives were approximated here using the so-called "1/6 trick" described by Claerbout (1985, p. 262). A value of 1/12 was used here because it yields less phase error than the value 1/6 for the 65-degree approximation.

Implicit extrapolators, in principle, are capable of high accuracy for very high propagation angles. Figure 8 shows contours of phase error for a "90-degree" implicit extrapolator. This extrapolator is obtained through a partial fraction expansion of the square-root in equation (1), as suggested by Ma (1981) and developed by Lee and Suh (1985). The computational cost of this extrapolator is approximately five times that of the 65-degree extrapolator. Again, note the frequency dependence of the phase error contours in Figure 8, which implies that small spatial sampling intervals are required to obtain 90-degree accuracy.

MIGRATION IMPULSE RESPONSES

To further test the stable explicit extrapolators derived in Appendix A, a migration program was developed based on those extrapolators. Figure 9 exhibits migration impulse responses for a 19-coefficient stable explicit extrapolator. The input to the migration was a section containing just three non-zero samples. In this example, spatial sampling intervals $\Delta z = \Delta x = 10$ m, time sampling interval $\Delta t = 10$ ms, and half-velocity = 1 km/s. The maximum (Nyquist) frequency is 50 Hz = $1/(2\Delta t)$. Therefore, these data contain normalized frequencies ranging from 0.0 to 0.5, the same range represented in Figures 6 through 8. These parameters are representative of those one might encounter in processing recorded seismic data.

Note that steep dips (high propagation angles) are attenuated in Figure 9. Those dips that are present are correctly positioned along concentric semicircles with centers at the origin. No visible dispersion of low and high frequencies is exhibited by these impulse responses. Figure 10 illustrates the benefit of increasing the number of coefficients in stable explicit extrapolators from 19 to 39. Increasing the number of coefficients by roughly a factor of 2 has increased the dip limit of stable explicit extrapolators by about 15 degrees. Again, note that no visible dispersion of low and high frequencies is exhibited by these impulse responses. As indicated in Figure 6, and confirmed in Figure 10, the phase accuracy of stable explicit extrapolators is more or less independent of frequency.

For comparison, a "65-degree" implicit migration yields the impulse responses shown in Figure 11. Note that the accuracy of this implicit method is frequency dependent. High frequencies are mis-positioned at steep dips, as suggested by the phase errors contoured in Figure 7. Also, note the heart-shaped character of the impulse responses. The particularly strong cusp at the center of each heart is dispersed

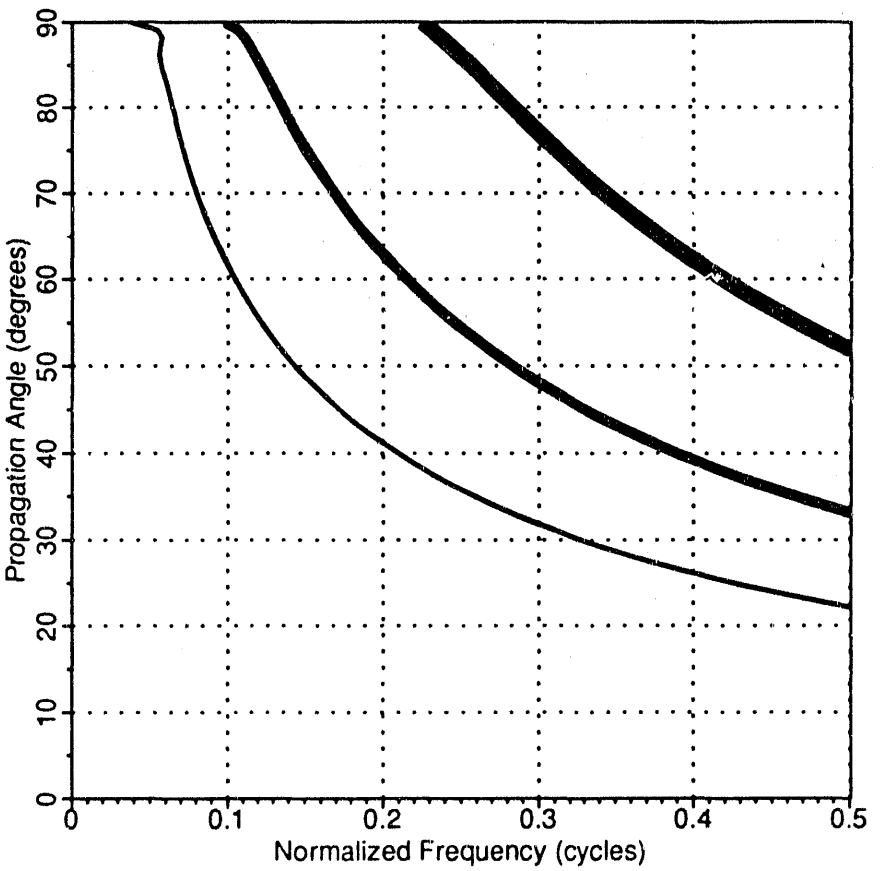

FIG. 8. Phase error for a so-called 90-degree implicit extrapolator. Compare with Figures 6 and 7. Error is contoured as a function of normalized frequency and propagation angle (measured from vertical). Normalized (dimension-less) frequency is frequency (Hz) times the horizontal sampling interval (km) divided by velocity (km/s). Contour values are $-\pi/1000$ (thin), $-\pi/100$ (medium), and $-\pi/10$ (thick).

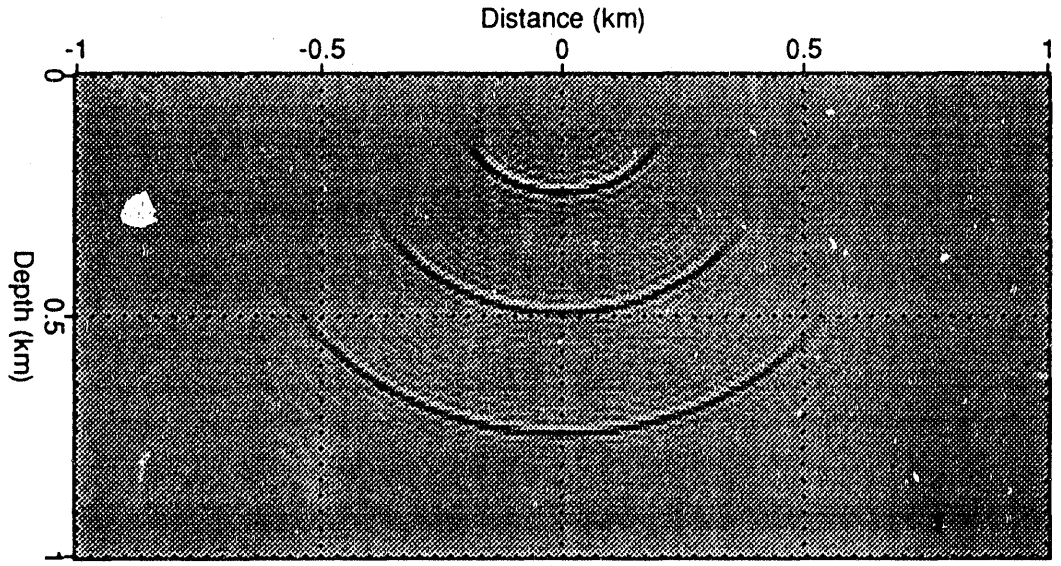

FIG. 9. Impulse responses of migration via 19-coefficient stable explicit extrapolators. Steep dips are attenuated, but dips remaining are correctly positioned along concentric semicircles with centers at the origin, with no visible dispersion of low and high frequencies.

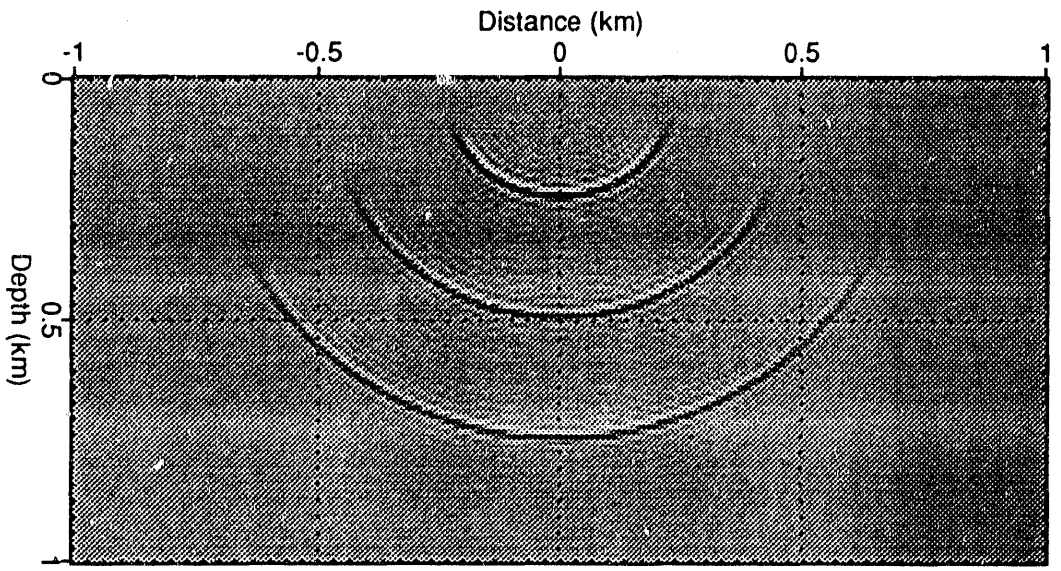

FIG. 10. Impulse responses of migration via 39-coefficient stable explicit extrapolators. Comparision with Figure 9 indicates that longer extrapolators yield steeper dips. As for Figure 9, note that the impulse responses are correctly positioned along concentric semicircles with centers at the origin, with no visible dispersion of low and high frequencies.

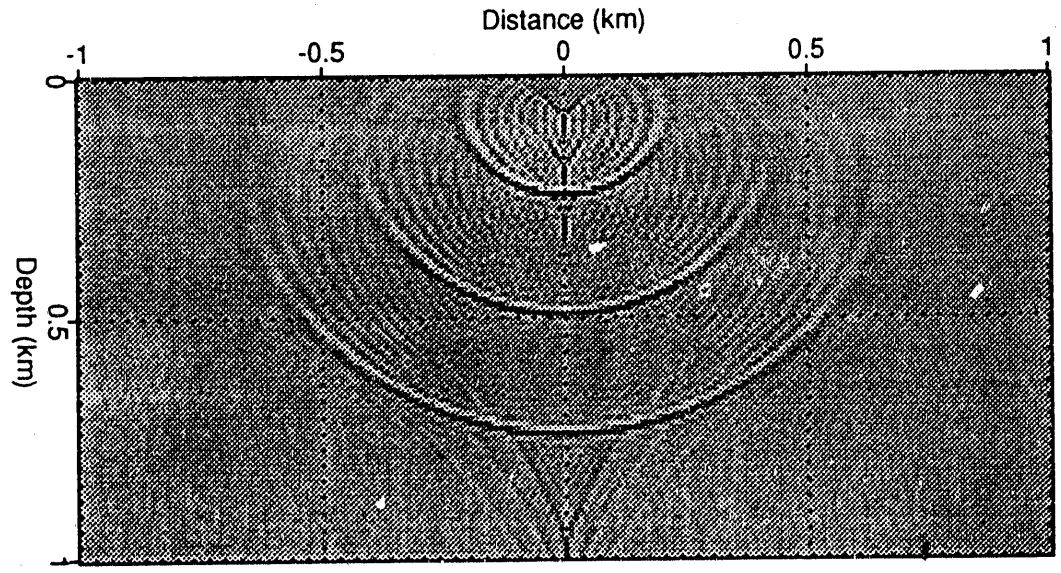

FIG. 11. Impulse responses of migration via 65-degree implicit extrapolators. Note the dispersion of low and high frequencies at steep dips. The heart-like shape of these impulse responses is dispersed evanescent energy not attenuated by implicit extrapolation. Compare with Figures 9 and 10.

evanescent energy contained in the impulses input to the migration. (See Claerbout, p. 247.) Unlike the stable explicit extrapolation filters described here, implicit extrapolation filters do not naturally attenuate this evanescent energy. In other words, implicit extrapolation filters do not know when to quit.

A DEPTH MIGRATION EXAMPLE

Explicit wavefield extrapolation is easy to incorporate in depth migration, which must handle lateral velocity variations. As suggested by Holberg (1988), one first computes a table of extrapolators for a typical range of normalized frequencies. Lateral velocity variations in extrapolating from one depth to the next are then handled by choosing the extrapolator most appropriate for each extrapolated sample. In other words, lateral velocity variations are handled by a lateral varying filter.

To illustrate this application of stable explicit extrapolators, I used finite-difference modeling of an exploding reflector for the velocity model shown in Figure 12 to compute the synthetic zero-offset section shown in Figure 13. Migrated images of the subsurface, computed using both 39-coefficient explicit and 65-degree implicit depth migrations are shown in Figures 14 and 15, respectively. Both the explicit and implicit depth migrations successfully image the horizontal (exploding) reflector located beneath the low-velocity lens at a depth of 3 km, between 2 and 4 km. Due to the lack of high frequencies in the synthetic data, the implicit method exhibits little frequency dispersion in this example.

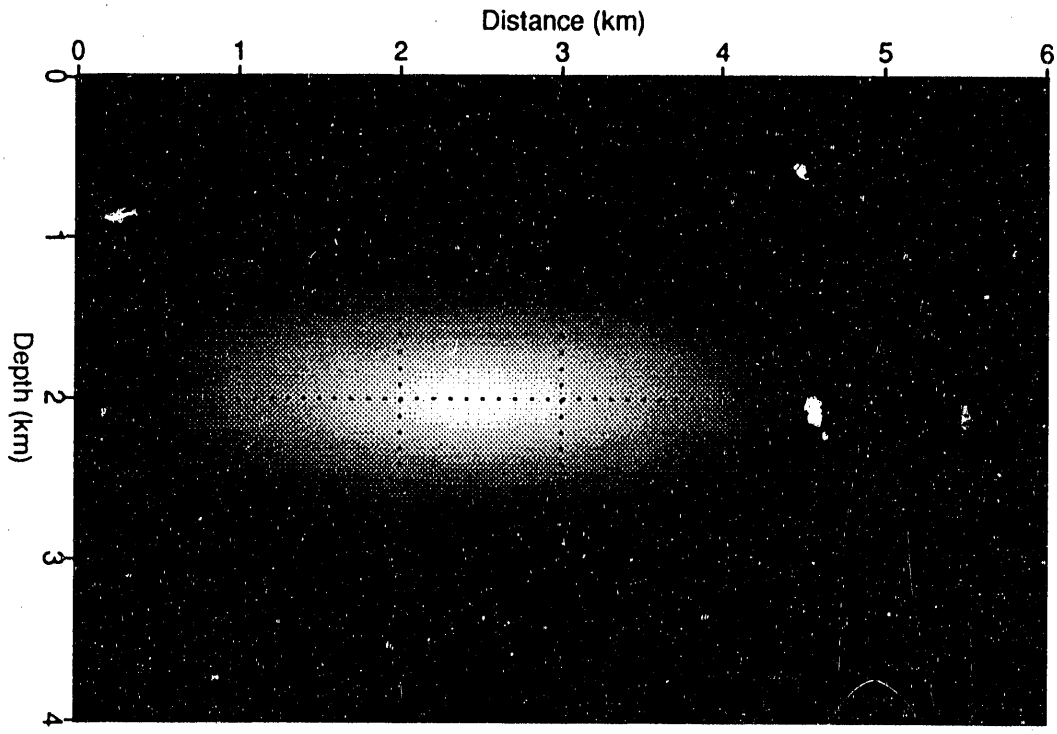

FIG. 12. Velocity model used to compute a synthetic zero-offset section via finite-difference modeling. Black shading corresponds to a velocity of 2 km/s. White shading (at the center of the lens) corresponds to a velocity of 1 km/s.

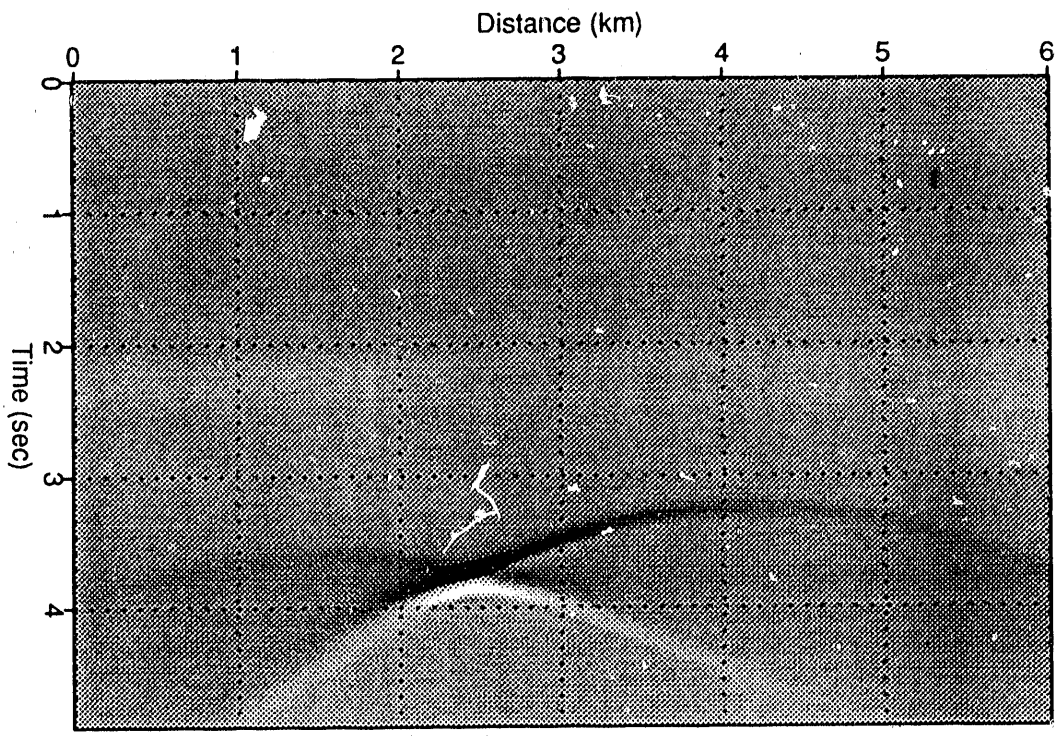

FIG. 13. Synthetic zero-offset section corresponding to an exploding reflector located at a depth of 3 km, centered laterally between 2 and 4 km, for the velocity model in Figure 12. Note that the low-velocity lens has focused the wavefield laterally between 2 and 3 km.

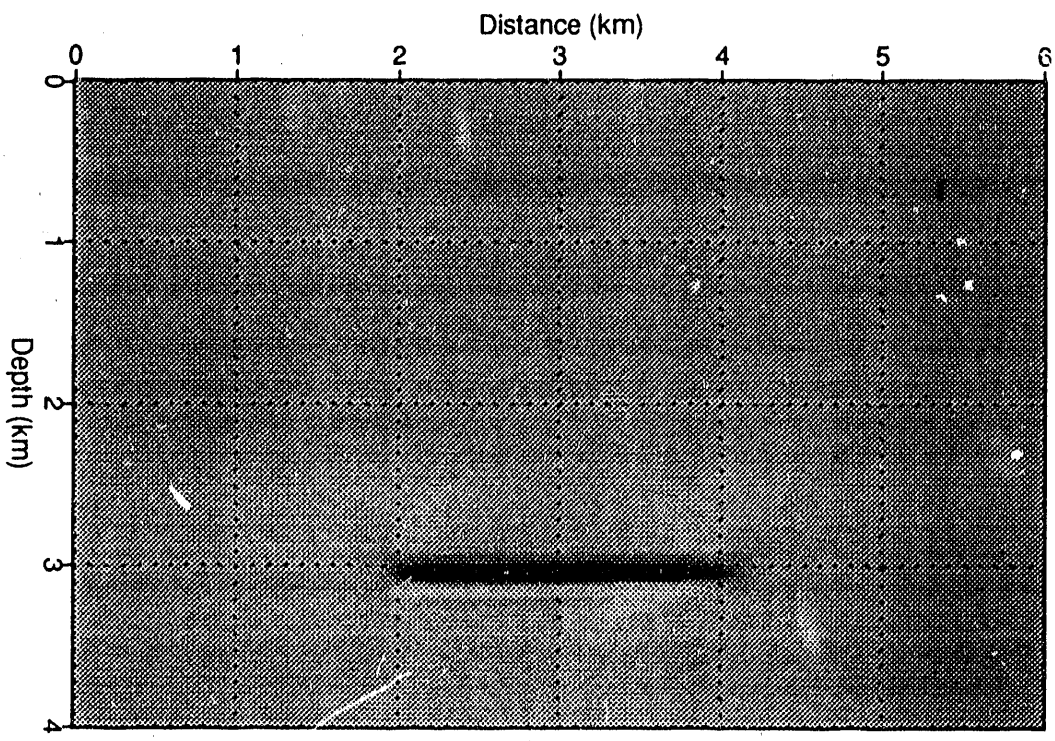

FIG. 14. Depth migration via 39-coefficient stable explicit extrapolation of the synthetic zero-offset section displayed in Figure 13. The exploding reflector has been properly imaged at a depth of 3 km, centered laterally betwee 2 and 4 km. Compare with Figure 15.

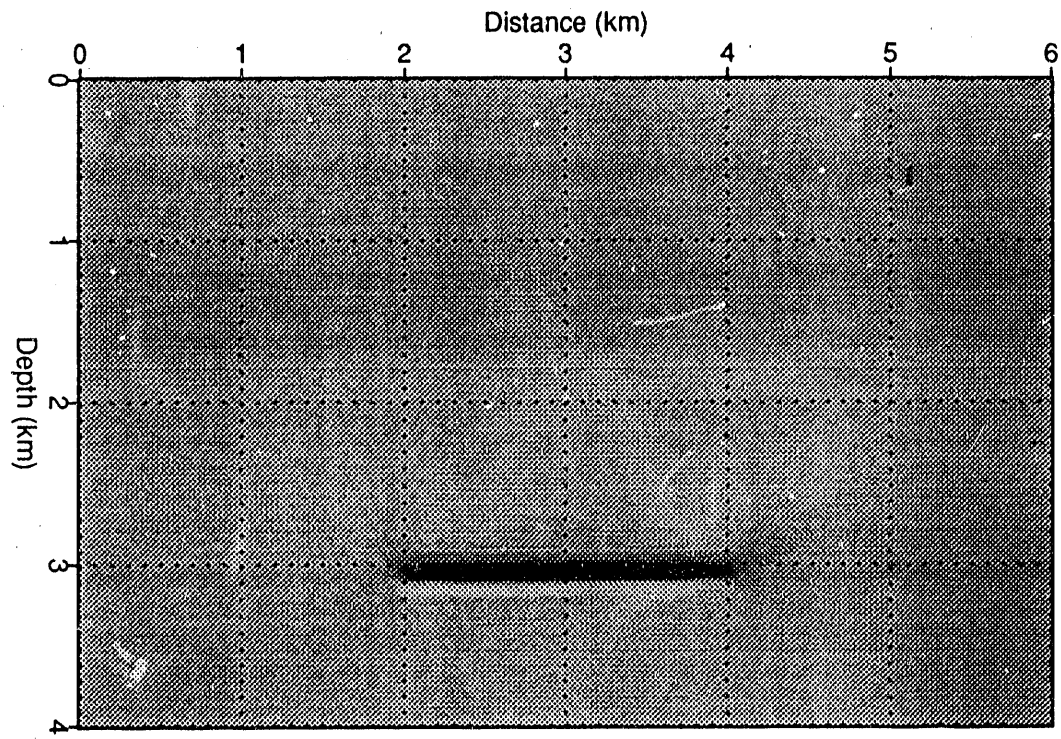

FIG. 15. Depth migration via so-called "65-degree" implicit extrapolation of the synthetic zero-offset section displayed in Figure 13. The exploding reflector has been properly imaged at a depth of 3 km, centered laterally between 2 and 4 km. Compare with Figure 14.

CONCLUSIONS

Stable explicit filters for depth extrapolation of seismic wavefields may be derived through a modification of the conventional Taylor series method. The modified Taylor series method describe here yields extrapolators with maximally-flat amplitude spectra in their passband, while ensuring that no spectral components in the wavefield are amplified by an factor greater than one.

The price for stability is increased phase error. The stable explicit extrapolators described here exhibit more phase error than do unstable extrapolators. Phase error in stable explicit extrapolators may be reduced by increasing the number of coefficients in the extrapolation filter.

For low normalized frequencies, implicit extrapolators (Figures 7 and 8) are more accurate than the 39-coefficient stable explicit extrapolator (Figure 6) described here. However, the small spatial sampling intervals required to obtain high phase accuracy in implicit extrapolation imply that this accuracy is rarely achieved in practice. Over the wide range of normalized frequencies likely to be encountered in practice, stable explicit extrapolators outperform implicit ones.

The method presented here for deriving stable explicit extrapolators is in no formal sense optimal. It is only guaranteed to yield stable extrapolators. In my limited experience with alternative methods for designing stable extrapolators, the method presented here produced the least phase error while ensuring stability. Nevertheless, a simple method for designing optimal (in some sense) stable explicit extrapolators would be preferred over the method presented here.

ACKNOWLEDGMENTS

Thanks to Ken Larner for his critical reading of the first draft of this paper. Financial support for this work was provided in part by the United States Department of Energy, Grant Number DE-FG02-89ER14079. (This support does not constitute an endorsement by DOE of the views expressed in this paper.) Support was also provided by the members of the Consortium Project on Seismic Inverse Methods for Complex Structures at the Center for Wave Phenomena, Colorado School of Mines.

REFERENCES

Blacquière, G., Debeye, H. W. J., Wapenaar, C. P. A., and Berkhout, A. J., 1989, 3D table-driven migration: Geophys. Prosp., **37**, 925–958.

Claerbout, J. F., 1985, Imaging the earth's interior: Blackwell Scientific Publications.

Holberg, O., 1988, Towards optimum one-way wave propagation: Geophys. Prosp., **36**, 99–114.

Kaiser, J. F., 1979, Design subroutine (MXFLAT) for symmetric FIR lowpass digital filters with maximally-flat pass and stop bands, in Digital Signal Processing

Committee of the IEEE ASSP Soc., Programs for Digital Signal Processing: IEEE Press, 5.3-1–5.3-6.

Lee, M. W., and Suh, S. Y., 1985, Optimization of one-way wave equations: Geophysics, **50**, 1634-1637.

Ma, Z., 1981, Finite-difference migration with higher-order approximation: Presented at the 1981 joint meeting of the China Geophysical Society and Soc. of Expl. Geophys., Beijing, China.

Yilmaz, O., 1987, Seismic Data Processing: Soc. of Expl. Geophysics.

APPENDIX A: DERIVATION OF STABLE EXTRAPOLATORS

The desired Fourier transform of the extrapolation filter is defined by

$$D(k) \equiv e^{i\frac{\Delta z}{\Delta x}\left[\left(\frac{\omega/\Delta x}{v}\right)^2 - k^2\right]^{1/2}}, \tag{A-1}$$

where ω denotes frequency (in radians per unit time), v denotes velocity, and Δz and Δx denote vertical and horizontal spatial sampling intervals, respectively. Wavenumber k (measured in radians per sample in the x direction) is normalized such that any distance quantity is measured in terms of the number of horizontal sampling intervals Δx. With this normalization, two dimension-less constants, $\Delta z/\Delta x$ and $\omega \Delta x/v$, will uniquely determine an extrapolation filter with a Fourier transform $H(k)$ approximating the desired transform $D(k)$.

Let h_n denote the N complex coefficients of a finite-length extrapolation filter. Because the extrapolation filter is symmetric (both the real and imaginary parts are even), N should be an odd number. The coefficient index n is bounded by $-(N-1)/2 \le n \le (N-1)/2$, and the filter is completely specified by only $(N+1)/2$ complex coefficients. Define the Fourier transform of the extrapolation filter by

$$\begin{aligned} H(k) &\equiv \sum_{n=\frac{-N+1}{2}}^{\frac{N-1}{2}} h_n e^{-ikn} \\ &= \sum_{n=0}^{\frac{N-1}{2}} (2 - \delta_{n0}) h_n \cos(kn), \end{aligned}$$

where δ_{n0} is the Kronecker delta function defined by

$$\delta_{n0} \equiv \begin{cases} 1, & \text{if } n = 0; \\ 0, & \text{otherwise.} \end{cases}$$

In the conventional Taylor series method of designing the extrapolation filter h_n, the $(N+1)/2$ distinct complex coefficients would be determined by equating derivatives of $H(k)$, the actual transform, with those of $D(k)$, the desired transform. In particular, because the extrapolation filter is symmetric and we want the filter to be exact for waves propagating vertically, we would match the first $(N+1)/2$ *even*

derivatives at $k = 0$. Unfortunately, this most straightforward application of the Taylor series method yields an unstable extrapolation filter, a filter for which $|H(k)| > 1$ for some wavenumbers k.

To obtain a stable filter, we must attempt to match fewer than $(N+1)/2$ derivatives and let the remaining degrees of freedom in the filter be exploited to guarantee $|H(k)| \leq 1$. In this modified Taylor series method, let the coefficients of the filter be represented as a sum of M weighted basis functions:

$$h_n = \sum_{m=0}^{M-1} c_m b_{mn}, \tag{A-2}$$

where, for reasons given below, a good choice for the basis functions is

$$b_{mn} = (2 - \delta_{m0}) \cos\left(\frac{2\pi mn}{N}\right). \tag{A-3}$$

Instead of determining $(N+1)/2$ complex filter coefficients h_n, we will determine M complex weights c_m. For stability, the number, M, of weights must be less than the number, $(N+1)/2$, of filter coefficients. Therefore, we will match only the first M even derivatives of the desired and actual Fourier transforms, using the remaining $(N+1)/2 - M$ degrees of freedom to guarantee stability.

In terms of the weights c_m to be determined, the Fourier transform of the extrapolation filter is

$$H(k) = \sum_{m=0}^{M-1} c_m (2 - \delta_{m0}) \sum_{n=0}^{\frac{N-1}{2}} (2 - \delta_{n0}) \cos\left(\frac{2\pi mn}{N}\right) \cos(kn) \tag{A-4}$$

$$= \sum_{m=0}^{M-1} c_m B_m(k), \tag{A-5}$$

where

$$B_m(k) \equiv (2 - \delta_{m0}) \sum_{n=0}^{\frac{N-1}{2}} (2 - \delta_{n0}) \cos\left(\frac{2\pi mn}{N}\right) \cos(kn) \tag{A-6}$$

are the Fourier transformed basis functions. Matching the l'th even derivative at $k = 0$, we obtain the linear equation

$$\sum_{m=0}^{M-1} c_m B_m^{(2l)}(0) = D^{(2l)}(0), \tag{A-7}$$

where

$$B_m^{(2l)}(0) = (2 - \delta_{m0})(-1)^l \sum_{n=0}^{\frac{N-1}{2}} (2 - \delta_{n0}) \cos\left(\frac{2\pi mn}{N}\right) n^{2l}.$$

By matching M such even derivatives, for $l = 0, 1, \ldots, M-1$, we obtain a system of M linear equations for the unknown weights c_m. After solving this linear system for

the weights c_m, we may use equations (A-2) and (A-3) to compute the extrapolation filter coefficients h_n.

In practice, the derivatives $D^{2l}(0)$ in the Taylor series expansion of the desired transform $D(k)$ [equation (A-1)] are best obtained with the help of a computer. For large l, expressions for these derivatives become unwieldy, but they can be expressed in terms of the constants $\Delta z/\Delta x$ and $\omega\Delta x/v$, and a table of numerical coefficients. In computing the extrapolation filters illustrated in this paper, I used Mathematica (Wolfram, 1988), a widely available computer program, to generate and store in a file the table of coefficients representing the first 40 terms of the Taylor series of the desired transform $D(k)$. This file, in turn, was then directly included during compilation of the computer program (written in the C programming language) that computed the extrapolation filter coefficients.

The stability of the extrapolation filters derived via this modified Taylor series method lies in the definition of the basis functions b_{mn} in equation (A-3). Each of these basis functions, corresponding to $m = 0, 1, \ldots, M-1$, represents a particular range of wavenumbers k, with $m = 0$ representing the wavenumbers centered at $k = 0$. To see this, we analytically compute the Fourier transform of each basis function, according to equation (A-6). The Fourier transform of the m'th basis function is

$$B_m(k) = \left(1 - \frac{\delta_{m0}}{2}\right) \left\{ \frac{\sin\left[\frac{N}{2}(k + \frac{2\pi m}{N})\right]}{\sin\left[\frac{1}{2}(k + \frac{2\pi m}{N})\right]} + \frac{\sin\left[\frac{N}{2}(k - \frac{2\pi m}{N})\right]}{\sin\left[\frac{1}{2}(k - \frac{2\pi m}{N})\right]} \right\}. \qquad \text{(A-8)}$$

These Fourier transformed basis functions are plotted in Figure A-1, for $M = 6$ and $N = 19$. For large N, each of the transforms in equation (A-8) is approximately equal to the sum of two sinc functions.

In the example illustrated in Figure A-1, four of the $(N+1)/2 = 10$ degrees of freedom in the extrapolation filter are used to place four zeros in its Fourier transform for high wavenumbers k. Recall equation (A-4), which states that the Fourier transform of the extrapolation filter $H(k)$ is just a weighted sum of the Fourier transforms of the basis functions $B_m(k)$. Therefore, regardless of the weights c_m computed by matching derivatives in the modified Taylor series method, the Fourier transform of the extrapolation filter will be forced to zero at four high wavenumbers k. It is at these higher wavenumbers that extrapolation filters derived via the conventional Taylor series method are most unstable. In the modified Taylor series method, forcing zeros in the transform at these high wavenumbers makes the extrapolation filter stable for all wavenumbers.

Unfortunately, I do not know how to determine the number of zeros necessary to ensure stability for a given filter length N and constants $\Delta z/\Delta x$ and $\omega\Delta x/v$, without simply testing different M, starting with $M = (N-1)/2$ and decreasing M until a stable extrapolation filter is found. Furthermore, I cannot prove that such a stable filter even *exists*; all I have shown is that the extrapolation filter will have $(N+1)/2 - M$ uniformly spaced zeros at the high wavenumbers in its Fourier transform. I merely make the conjecture that such a stable filter always exists, that

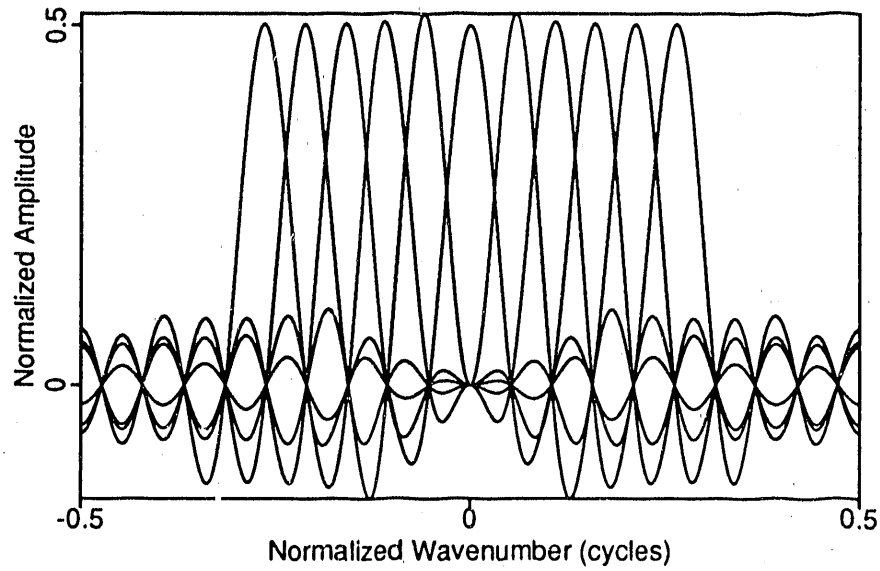

FIG. A-1. Fourier transforms of basis functions for $M = 6$ and $N = 19$. Note that, in this example, there are $(N + 1)/2 - M = 4$ uniformly spaced zeros at the high wavenumbers. These zeros attenuate evanescent waves and ensure stability of the corresponding extrapolation filter. The Fourier transform of the extrapolation filter is just a weighted sum of these sinc-like functions.

a suitable M can always be found, based on my experience in deriving filters via this modified Taylor series method.

I have also found, again empirically, that stable filters derived using this modified Taylor series method tend to have their zeros at wavenumbers corresponding to evanescent waves, inhomogeneous waves for which $|k| > |\omega \Delta x / v|$. This feature is illustrated in Figure 1 of the text. The zeros tend to attenuate evanescent waves and waves propagating at angles for which the extrapolation filter has significant error in phase, as illustrated by Figures 5 and 6.

The modification described above to the conventional Taylor series method is just one among many possible modifications. One likely alternative method that I have tested is to solve $(N + 1)/2$ equations directly for the unknown filter coefficients h_n (without basis functions), with M of the equations used to match the first M even derivatives of $D(k)$ at $k = 0$ and the remaining $(N + 1)/2 - M$ equations used to zero the first $(N + 1)/2 - M$ even derivatives of the actual transform $H(k)$ at $k = \pi$. This method is analogous to the design of maximally-flat, zero-phase, finite-length, low-pass filters described by Kaiser (1979). Like the basis function method described above, this "maximally-flat" method is also guaranteed to yield a stable extrapolation filter for some choice of M. However, the phase errors obtained with the maximally-flat method exceed those obtained with the basis function method, particularly for low normalized frequencies.

END

DATE FILMED

11 / 30 / 90